Available online at www.sciencedirect.com
ScienceDirect
Signal Processing 87 (2007) 811–823
SIGNAL PROCESSING
www.elsevier.com/locate/sigpro

An efficient closed-form design method for cosine-modulated filter banks using window functions

Stuart W.A. Bergen, Andreas Antoniou*

Department of Electrical and Computer Engineering, University of Victoria, P.O. Box 3055 STN CSC, Victoria, BC, Canada V8W 3P6

Received 18 February 2006; received in revised form 2 August 2006; accepted 7 August 2006
Available online 1 September 2006

Abstract

An efficient closed-form method for designing M-channel cosine-modulated filter banks with prescribed stopband attenuation and channel overlap is proposed. The method employs the window technique for the prototype filter design and is based on empirical formulas that give the filter length and the window parameters that would satisfy the prescribed specifications. When compared with iterative methods, the proposed method significantly reduces the computational cost associated with the design making it a suitable candidate for applications where the design must be carried out in real or quasi-real time. Applications of the proposed method in the area of subband processing of speech, audio, and ECG signals are considered.

Keywords: Cosine-modulated filter banks; Nonrecursive (FIR) filter design; Window functions

1. Introduction

A fundamental system used in multirate applications is the M-channel maximally decimated filter bank. For cosine-modulated filter banks (CMFBs), the analysis and synthesis filters are cosine-modulated versions of a lowpass prototype filter which is typically designed to minimize three error components (amplitude distortion, phase distortion, and aliasing) that are inherent in the system. Maximally decimated filter banks with no reconstruction errors can be designed as perfect reconstruction (PR) CMFBs which are suited for applications such as lossless coding. For applications where errors are introduced at the subband level, as in lossy coding, the reconstructed signal is not a delayed replica of the input signal. For these applications, signal distortion caused by reconstruction errors is allowed provided that its level is insignificant relative to that caused by coding. Consequently, the PR condition can be relaxed in order to achieve other filter bank properties such as increased stopband attenuation in the subbands.

Recent applications of filter banks include perceptual coding of digital audio [1] and heartbeat detection in ECG signals [2]. In perceptual audio coding, filter banks with high stopband attenuation, small channel overlap, and efficient resolution switching can improve sound quality. In ECG heartbeat detection, filter banks with adjustable stopband attenuation and efficient resolution switching

*Corresponding author. Tel.: +1 250 721 4780; fax: +1 250 721 6052.
E-mail addresses: sbergen@ece.uvic.ca (S.W.A. Bergen), aantoniou@ieee.org (A. Antoniou).

0165-1684/$ - see front matter © 2006 Elsevier B.V. All rights reserved.
doi:10.1016/j.sigpro.2006.08.003

are useful for analyzing ECG signals of different patients. Consequently, fast, flexible, and efficient filter-bank design methods that yield prescribed stopband attenuation and channel overlap are highly desirable.

An early design method for CMFBs was proposed by Creusere and Mitra [3] who used the weighted-Chebyshev method [4] to design the prototype filter. Next, Lin and Vaidyanathan [5] used the Kaiser window approach [4] to design the prototype filter while, recently, Cruz-Roldán et al. [6] modified this method to include other windows. These methods are iterative and, therefore, they are not suitable for applications where the design must be carried out in real or quasi-real time. For such applications a closed-form window method is preferred.

In this paper, a closed-form and computationally efficient method for designing prototype filters for M-channel CMFBs that achieve a prescribed stopband attenuation and channel overlap is proposed. The paper is structured as follows. Section 2 reviews the design of CMFBs using the window method. Section 3 describes the application of the method in terms of the Kaiser [4], Saramäki [7], and ultraspherical [8] window functions. Section 4 examines the performance of CMFBs designed with the proposed method and compares the designs obtained with designs obtained with other methods. Section 5 considers applications of the proposed method in the area of subband processing of speech, audio, and ECG signals. Section 6 provides concluding remarks.

2. Design of CMFBs using the window method

Fig. 1 shows the generalized parallel structure for an M-channel maximally decimated filter bank. The input–output relations for a CMFB are given by [9]

$$Y(z) = T_0(z)X(z) + \sum_{l=1}^{M-1} T_l(z)X(zW_M^l), \tag{1}$$

where $W_M = e^{-j2\pi/M}$ and

$$T_l(z) = \frac{1}{M}\sum_{k=0}^{M-1} F_k(z)H_k(zW_M^l) \tag{2}$$

for $l = 0, 1, \ldots, M-1$. In Eq. (1), $T_0(z)$ is the transfer function of the filter bank, $T_l(z)$ for $1 \leqslant l \leqslant M-1$ are the aliasing transfer functions, and $H_k(z)$ and $F_k(z)$ are the individual transfer functions of the analysis and synthesis filters, respectively. Assuming filters of length N, the impulse responses for the analysis and synthesis filters are given by [9]

$$h_k(n) = 2h_p(n)\cos\left[\omega_k\left(n - \frac{N-1}{2}\right) + \theta_k\right], \tag{3}$$

$$f_k(n) = h_k(N-1-n) \tag{4}$$

for $k = 0, 1, \ldots, M-1$ where $h_p(n)$ is the impulse response of a linear-phase nonrecursive prototype filter of length N and

$$\omega_k = \frac{(2k+1)\pi}{2M} \quad \text{and} \quad \theta_k = (-1)^k\frac{\pi}{4}. \tag{5}$$

Three types of errors are encountered in filter banks, namely, phase (or delay) distortion, amplitude distortion, and aliasing distortion. In CMFBs of the type being considered, phase distortion is eliminated through the use of linear-phase filters. Consequently, these filter banks are characterized by the error in the amplitude response

$$e_m(\omega) = 1 - |T_0(e^{j\omega})| \quad \text{for } \omega \in [0, \pi] \tag{6}$$

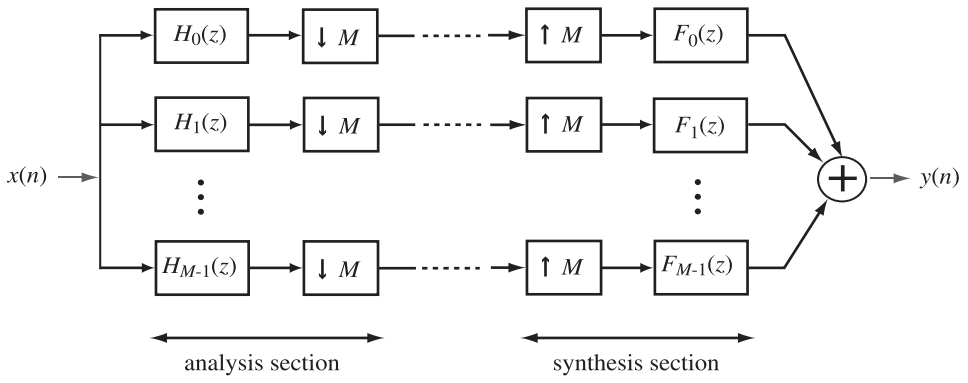

Fig. 1. M-channel maximally decimated filter bank.

the worst-case aliasing distortion

$$e_a(\omega) = \max_{1 \leqslant l \leqslant M-1} |T_l(e^{j\omega})| \quad \text{for } \omega \in [0, \pi] \tag{7}$$

and the total aliasing distortion

$$e_{ta}(\omega) = \left[\sum_{l=1}^{M-1} |T_l(e^{j\omega})|^2 \right]^{1/2} \quad \text{for } \omega \in [0, \pi]. \tag{8}$$

Small reconstruction errors can be achieved by designing the lowpass prototype filter using the window technique, i.e., by letting

$$h_p(n) = w(n) h_{id}(n), \tag{9}$$

where $w(n)$ is a window function of length N and

$$h_{id}(n) = \begin{cases} \omega_c/\pi & \text{for } n = 0, \\ \dfrac{\sin \omega_c n}{n\pi} & \text{for } n \neq 0, \end{cases} \tag{10}$$

where ω_c is the cutoff frequency. Prescribed stopband attenuation and channel overlap can be achieved by requiring the nonrecursive (noncausal) lowpass prototype filter to satisfy the specifications

$$\begin{aligned} &1 - \delta_p \leqslant H_p(e^{j\omega}) \leqslant 1 + \delta_p \quad \text{for } |\omega| \in [0, \omega_p], \\ &-\delta_a \leqslant H_p(e^{j\omega}) \leqslant \delta_a \quad \text{for } |\omega| \in [\omega_a, \omega_s/2], \end{aligned} \tag{11}$$

where δ_p and δ_a are the passband and stopband ripples and ω_p and ω_a are the passband and stopband edge frequencies, respectively. For filters designed using the window technique, the passband ripple turns out to be approximately equal to the stopband ripple, i.e., $\delta_p \approx \delta_a$. Consequently, the prototype filter can be designed to achieve a stopband attenuation A_a specified in dB by setting the stopband ripple to

$$\delta_a = 10^{0.05 A_a}. \tag{12}$$

The transition bandwidth of the filter is given by

$$B_t = \omega_a - \omega_p \tag{13}$$

and its cutoff frequency is $\omega_c = (\omega_p + \omega_a)/2$. Closed-form methods for constructing windows that achieve prescribed lowpass specifications can be found in [4,7,8] for the Kaiser, Saramäki, and ultraspherical windows, respectively.

3. Efficient design of prototype filter

The conditions for approximate reconstruction in a filter bank can be stated in terms of the amplitude responses of the prototype filter and the filter bank which are given by [9]

$$|H_p(e^{j\omega})| \approx 0 \quad \text{for } |\omega| > \pi/M \tag{14}$$

and

$$|T_0(e^{j\omega})| = \frac{1}{M} \sum_{k=0}^{2M-1} |H_p(e^{j(\omega - k\pi/M)})|^2 \approx 1, \tag{15}$$

respectively. The accuracy of the first approximation determines the magnitude of the aliasing errors in Eqs. (7) and (8) while the accuracy of the second approximation determines the amplitude-response error in Eq. (6).

A CMFB can be characterized by the stopband attenuation of the lowpass prototype filter, A_a, in dB and the stopband edge frequency

$$\omega_a = \frac{(1+\rho)\pi}{2M}, \tag{16}$$

where ρ is a design parameter called the *roll-off factor* [10]. Parameter ρ influences the overlap between subbands as illustrated in Fig. 2. In particular, if $0 < \rho \leqslant 1$ then each subband is overlapped by its adjacent subbands, i.e., by one subband on each side. If $1 < \rho \leqslant 2$ then each subband is overlapped by four subbands, i.e., two subbands on each side.

The amplitude-response error is reduced when $|T_0(e^{j\omega})|$ in Eq. (15) is constant. This can be accomplished by designing the prototype filter so that $|H_p(e^{j\omega})|^2 \approx \frac{1}{2}$ at $\omega = \pi/2M$, i.e.,

$$|H_p(e^{j\pi/2M})| \approx \tfrac{1}{\sqrt{2}}. \tag{17}$$

With A_a, ρ, and M specified, the required design can be obtained by selecting the passband edge frequency ω_p so that Eq. (17) is satisfied. This can be accomplished by solving the optimization problem

$$\begin{aligned} \min_{\omega_p} \quad & F = [|H_p(e^{j\pi/2M})| - 1/\sqrt{2}]^2 \\ \text{s.t.} \quad & 0 \leqslant \omega_p \leqslant \pi/2M \end{aligned} \tag{18}$$

using a simple one-dimensional optimization algorithm such as dichotomous, Fibonacci, or golden section line searches, as outlined in [11]. For each iteration, the computation of the objective function requires the re-estimation of the filter length, the window parameters, the window coefficients, and the infinite-duration impulse response of the filter. Closed-form methods for these tasks are described in [4,7,8] for the Kaiser, Saramäki, and ultraspherical windows, respectively.

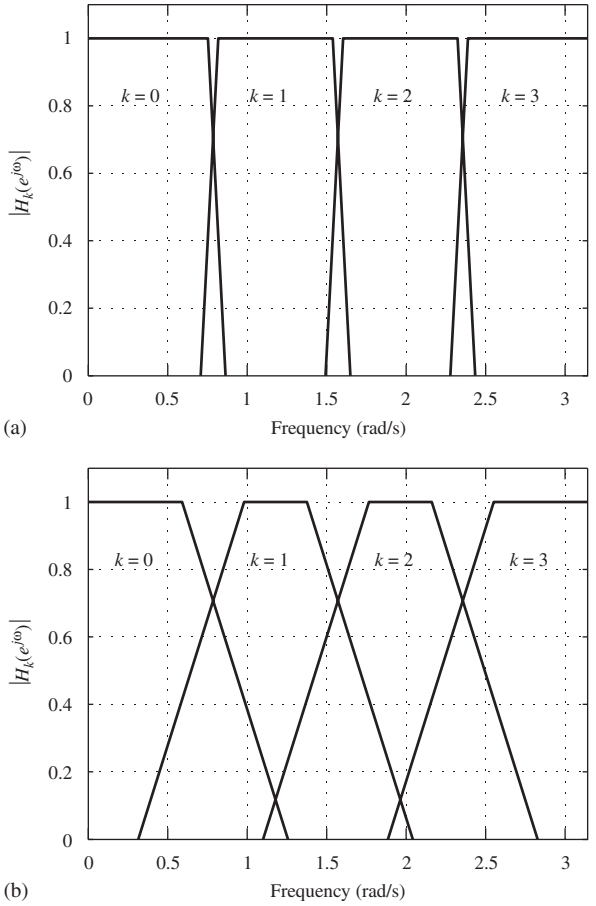

Fig. 2. Amplitude responses for the idealized analysis filters for a 4-channel CMFB for (a) $\rho = 0.2$ and (b) $\rho = 1.2$.

The above design method was used to deduce empirical formulas that can be used to estimate the passband edge frequency ω_p that minimizes the objective function in Eq. (18). Fig. 3 shows plots of the objective function vs. the performance measure

$$D = \omega_p \times \frac{2M}{\pi} \tag{19}$$

for various values of ρ where D is a normalized measure of the passband edge frequency. By examining a large number of designs it was observed that the value of D for the optimal solution for a given ρ remains constant to within 0.01% deviation regardless of the number of subbands, i.e., the minimum value of F in Eq. (18) vs. D does not change as M changes. Fig. 4 shows plots of the resulting optimized values of D vs. ρ for various values of A_a. Through curve fitting, an empirical

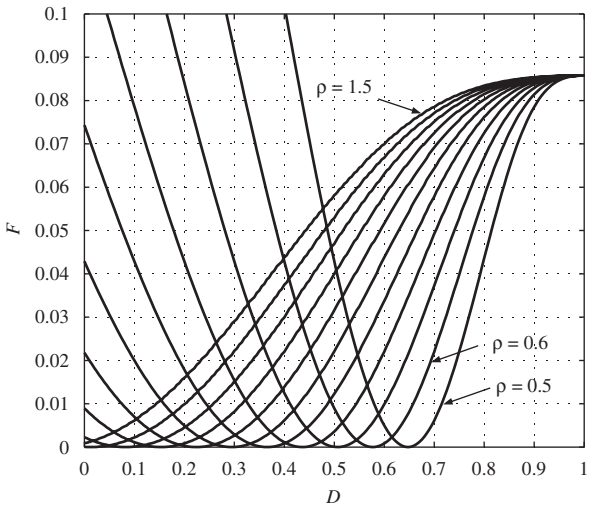

Fig. 3. Values of the objective function over the range $0 \leqslant D \leqslant 1$ for various values of the roll-off factor ρ for the Kaiser window.

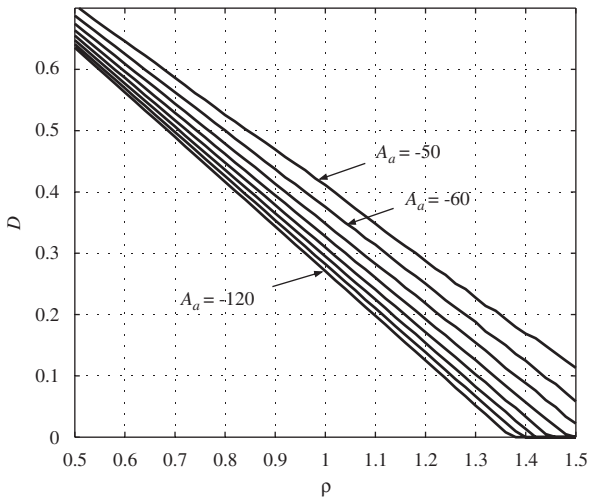

Fig. 4. Values of D that minimize the objective function over the range $0.5 \leqslant \rho \leqslant 1.5$ for various stopband attenuations for the Kaiser window.

formula was derived for D in the form

$$D = \begin{cases} a_1\rho^2 + b_1\rho + c_1 & \text{for } 0.5 \leqslant \rho < 1.0, \\ a_2\rho^2 + b_2\rho + c_2 & \text{for } 1.0 \leqslant \rho \leqslant 1.5. \end{cases} \tag{20}$$

The model coefficients for the values $A_a = \{-50, -60, -70, \ldots, -150\}$ for the Kaiser and ultraspherical windows are given in Table 1. Model coefficients for the Saramäki window have also been obtained but are not included for the sake of brevity. These coefficients can be used for all applications and their recalculation is unnecessary.

Table 1
Model coefficients for D for the (a) Kaiser window and (b) ultraspherical window in Eq. (20) ($0.5 \leqslant \rho \leqslant 1.5$)

A_a	a_1	b_1	c_1	a_2	b_2	c_2
(a)						
−50	$3.096E-2$	$-6.345E-1$	$1.015E+0$	$8.307E-2$	$-8.016E-1$	$1.130E+0$
−60	$2.150E-3$	$-6.286E-1$	$1.002E+0$	$-1.543E-2$	$-5.931E-1$	$9.838E-1$
−70	$-1.173E-3$	$-6.502E-1$	$9.998E-1$	$-1.909E-2$	$-6.043E-1$	$9.711E-1$
−80	$3.107E-4$	$-6.735E-1$	$1.000E+0$	$-3.959E-4$	$-6.738E-1$	$1.002E+0$
−90	$-1.839E-3$	$-6.880E-1$	$9.994E-1$	$-9.398E-3$	$-6.680E-1$	$9.866E-1$
−100	$1.504E-3$	$-7.074E-1$	$1.001E+0$	$7.341E-3$	$-7.237E-1$	$1.011E+0$
−110	$-7.255E-4$	$-7.167E-1$	$9.996E-1$	$1.756E-2$	$-7.601E-1$	$1.025E+0$
−120	$2.536E-3$	$-7.329E-1$	$1.001E+0$	$-9.054E-3$	$-7.085E-1$	$9.882E-1$
−130	$4.979E-4$	$-7.398E-1$	$1.000E+0$	$6.255E-3$	$-7.547E-1$	$1.010E+0$
−140	$2.707E-4$	$-7.484E-1$	$1.000E+0$	$-4.075E-3$	$-7.403E-1$	$9.964E-1$
−150	$-4.951E-4$	$-7.553E-1$	$9.999E-1$	$-1.072E-2$	$-7.322E-1$	$9.870E-1$
(b)						
−50	$4.247E-2$	$-6.463E-1$	$1.020E+0$	$1.091E-1$	$-8.717E-1$	$1.178E+0$
−60	$-1.146E-2$	$-6.098E-1$	$9.966E-1$	$-1.090E-2$	$-6.061E-1$	$9.942E-1$
−70	$-3.803E-3$	$-6.458E-1$	$9.993E-1$	$1.126E-2$	$-6.822E-1$	$1.021E+0$
−80	$-2.042E-4$	$-6.731E-1$	$1.001E+0$	$3.961E-3$	$-6.838E-1$	$1.008E+0$
−90	$-1.650E-3$	$-6.887E-1$	$1.000E+0$	$-6.863E-3$	$-6.757E-1$	$9.922E-1$
−100	$-2.006E-3$	$-7.028E-1$	$9.998E-1$	$2.577E-3$	$-7.131E-1$	$1.006E+0$
−110	$-4.775E-3$	$-7.110E-1$	$9.982E-1$	$-2.948E-4$	$-7.175E-1$	$1.000E+0$
−120	$1.256E-3$	$-7.301E-1$	$1.001E+0$	$-3.871E-3$	$-7.212E-1$	$9.971E-1$
−130	$-4.209E-4$	$-7.383E-1$	$1.000E+0$	$2.854E-4$	$-7.405E-1$	$1.002E+0$
−140	$6.519E-4$	$-7.488E-1$	$1.001E+0$	$7.473E-3$	$-7.655E-1$	$1.011E+0$
−150	$-8.206E-4$	$-7.548E-1$	$1.000E+0$	$-5.601E-4$	$-7.560E-1$	$1.001E+0$

The reason for this is that D is approximately independent of M as described earlier. However, the coefficients would need to be stored for applications where the filter bank has to be designed in real or quasi-real time but this is not a serious limitation nowadays. Estimates for D corresponding to values of A_a in the range $[-150, -50]$ are not included in Table 1 but can be determined using cubic spline interpolation in conjunction with Eq. (20).

The empirical formulas provide an accurate estimate of the optimal ω_p over a useful range of the system design parameters, namely, $M \in \{2, 3, \ldots, 1024\}$, $-150 \leqslant A_a \leqslant -50$, and $0.5 \leqslant \rho \leqslant 1.5$.

The above findings lead to a closed-form method for designing the prototype filter for an M-channel CMFB that achieves a prescribed stopband attenuation A_a in dB and a roll-off ratio ρ. The Kaiser, Saramäki, or ultraspherical window can be employed. An algorithm based on the Kaiser window case is as follows:

Algorithm 1. Design of prototype filter for CMFBs using the Kaiser window.

Step 1: Input M, A_a, and ρ.

Step 2: Calculate the stopband ripple, δ_a, using Eq. (12).

Step 3: Calculate the stopband edge frequency, ω_a, using Eq. (16).

Step 4: Calculate parameter D using Eq. (20) in conjunction with Table 1.

Step 5: Calculate the passband edge frequency, ω_p, using

$$\omega_p = D \times \frac{\pi}{2M}. \tag{21}$$

Step 6: Using parameters δ_a, ω_p, and ω_a, calculate the Kaiser window's parameters α and N and then its coefficients. Closed-form equations for both tasks are provided in [4].

Step 7: Calculate the relevant terms of the infinite-duration impulse response using Eq. (10) with $\omega_c = (\omega_p + \omega_a)/2$.

Step 8: Obtain the noncausal finite-duration impulse response for the prototype filter using Eq. (9).

Algorithms that can be used with the Saramäki and ultraspherical windows can be obtained by modifying Algorithm 1 in two locations. In Step 4, D in Eq. (20) is calculated using model coefficients that correspond to the Saramäki window (not included) and the ultraspherical window (Table 1).

Second, Step 6 requires equations that yield the window function's parameters and its coefficients. Closed-form equations for these tasks for the Saramäki and ultraspherical windows can be found in [7,8], respectively.

4. Comparisons

Below, we first compare the use of different windows such as the Kaiser, Saramäki, and ultraspherical windows in the proposed design method. Next we compare the proposed method with other known methods.

4.1. Comparison between windows

The proposed method was used to design a number of 32-channel CMFBs with a stopband attenuation of -100 dB. A CMFB satisfying these specifications can be used in the MPEG audio coder, and has been used on a number of occasions to compare different filter-bank design methods [3,5,6]. Designs were obtained with the proposed method using the Kaiser, Saramäki, and ultraspherical windows for different values of the roll-off factor ρ. Fig. 5 shows plots of the amplitude responses of the prototype filter, analysis filters, and the filter bank as well as the worst-case and total aliasing errors and the amplitude-response error for the filter bank designed using the proposed method with a Kaiser window and $\rho = 1.05$. Designs were also obtained using the Dolph–Chebyshev window but the performance achieved was not as good.

(1) *Reconstruction errors*: Table 2 lists the maximum reconstruction errors and the prototype filter length associated with a set of filter banks designed using the proposed method. Fig. 6 shows plots of the maximum reconstruction errors of filter banks designed with values of ρ over the range $0.5 \leqslant \rho \leqslant 1.5$. The plots show that when the subband overlap increases (larger values of ρ) the aliasing errors begin to increase significantly around the value of $\rho = 1.3$. On the other hand, amplitude distortion remains relatively constant over the entire range of ρ. The average percentage decrease in error provided by the Kaiser window over the Saramäki and ultraspherical windows was 11.7% and 12.2% for $\max|e_m(\omega)|$, 1.3% and 26.5% for $\max|e_a(\omega)|$, and 2.1% and 34.7% for $\max|e_{ta}(\omega)|$, respectively. On the average, the Kaiser window provides the smallest reconstruction errors although cases exist where the use of the Saramäki or ultraspherical window yields smaller reconstruction errors. For instance, when $\rho = 1.2$ the use of the Saramäki window yields a reduction in all of the maximum errors relative to the designs obtained using the Kaiser window as can be seen in Table 2.

(2) *Prototype filter length*: The length of the prototype filter is automatically selected in Step 6 of Algorithm 1 to be the lowest possible length that would satisfy the lowpass filter specifications δ_a, ω_p, and ω_a. The resulting filter length varies depending on the window employed. Use of the ultraspherical window provides an average decrease in the prototype filter length of 3.1% and 2.9% relative to the Kaiser and Saramäki windows, respectively. This is consistent with the results reported in [8], which indicate that the ultraspherical window yields lower-order filters than those designed using the Kaiser or Saramäki windows for a given set of lowpass filter specifications.

By virtue of the modulation process, the analysis and synthesis filters are of the same length as the prototype filter. As such, computational costs associated with the prototype filter length can increase quickly when the filter bank has a large number of subbands. In such applications, the use of the ultraspherical window can provide a substantial savings relative to the computational costs associated with the Kaiser window. In addition, prototype filters of shorter length reduce the delay of the filter bank, which may be of importance to some applications.

(3) *Design time of the prototype filter*: The design time of the prototype filter is essentially equal to the time it takes to compute the coefficients of the window function. Fig. 7 shows the computation time[1] required to evaluate the coefficients of the ultraspherical and Kaiser windows vs. the window length. The Saramäki window is a particular case of the ultraspherical window and, therefore, the amount of computation is the same as for the ultraspherical window. For the Kaiser window, the zeroth-order modified Bessel function of the first kind $I_0(x)$ was evaluated to an accuracy of $\varepsilon = 10^{-10}$. As can be seen, use of the ultraspherical window requires only a fraction of the computation required by the use of the Kaiser window typically of the order of 9%.

[1]The computation time of the design methods was measured using the MATLAB stopwatch commands *tic* and *toc* which return the total CPU time used to execute the code between the two commands.

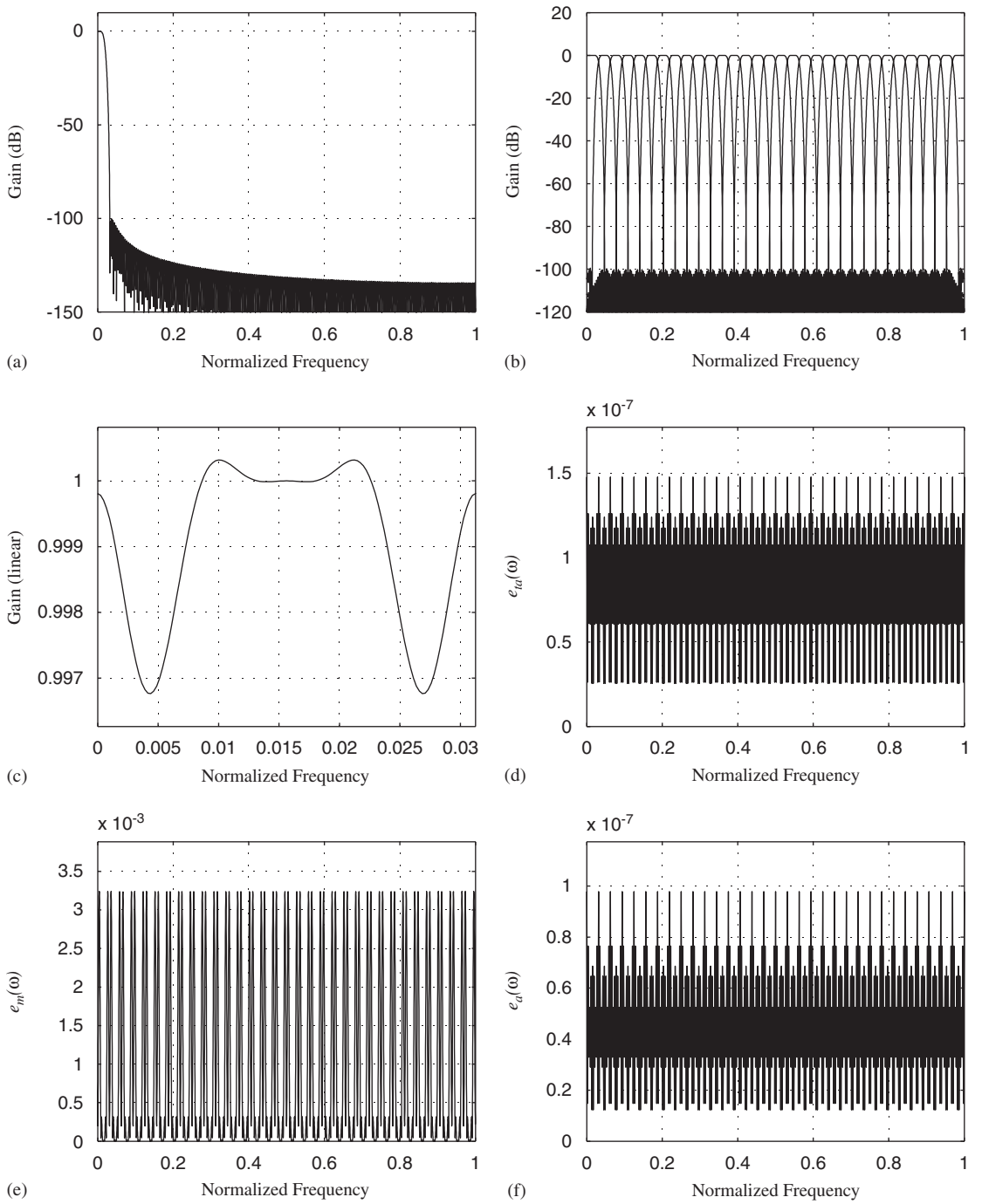

Fig. 5. Performance of the CMFB designed using the proposed method with $M = 32$, $A_a = -100$ dB, and $\rho = 1.05$ for the Kaiser window: (a) amplitude response of the prototype filter in dB; (b) amplitude responses of the analysis filters in dB; (c) $|T_0(e^{j\omega})|$ over $[0, \pi/M]$; (d) total aliasing error $e_{ta}(\omega)$; (e) amplitude-response error $e_m(\omega)$; and (f) worst-case aliasing error $e_a(\omega)$.

4.2. Comparison with other methods

The proposed method was used with the Kaiser window to design 16-channel CMFBs with $\rho = 1.00$ for stopband attenuations varying over the range $[-150, -50]$. The roll-off factor was chosen to be 1.00 so that only subbands which are immediately adjacent to one another overlap, i.e., for a given

Table 2
Reconstruction error comparison for the design example

Design method	N	$\max \lvert e_m(\omega)\rvert$	$\max \lvert e_a(\omega)\rvert$	$\max \lvert e_{ta}(\omega)\rvert$
Method in [3]	439	1.80×10^{-3}	6.13×10^{-7}	2.54×10^{-6}
Method in [5]	467	2.42×10^{-3}	2.67×10^{-7}	3.86×10^{-7}
Method in [6]	439	3.06×10^{-3}	1.85×10^{-7}	2.61×10^{-7}
Kaiser $\rho = 1.00$	483	3.13×10^{-3}	3.73×10^{-7}	5.52×10^{-7}
Kaiser $\rho = 1.05$	460	3.23×10^{-3}	9.78×10^{-8}	1.48×10^{-7}
Kaiser $\rho = 1.10$	439	3.40×10^{-3}	1.84×10^{-7}	2.60×10^{-7}
Kaiser $\rho = 1.20$	401	3.85×10^{-3}	2.38×10^{-7}	3.80×10^{-7}
Saramäki $\rho = 1.00$	482	3.90×10^{-3}	3.86×10^{-7}	5.63×10^{-7}
Saramäki $\rho = 1.05$	459	3.53×10^{-3}	9.13×10^{-8}	1.39×10^{-7}
Saramäki $\rho = 1.10$	438	3.90×10^{-3}	1.85×10^{-7}	2.62×10^{-7}
Saramäki $\rho = 1.20$	402	3.68×10^{-3}	2.29×10^{-7}	3.73×10^{-7}
Ultraspherical $\rho = 1.00$	468	3.85×10^{-3}	6.63×10^{-7}	9.44×10^{-7}
Ultraspherical $\rho = 1.05$	446	3.80×10^{-3}	1.58×10^{-7}	2.26×10^{-7}
Ultraspherical $\rho = 1.10$	425	4.41×10^{-3}	2.63×10^{-7}	4.34×10^{-7}
Ultraspherical $\rho = 1.20$	390	4.20×10^{-3}	4.56×10^{-7}	1.17×10^{-6}

subband two subbands (one on either side) will overlap (see Fig. 2). CMFBs satisfying the same specifications were designed using the methods of [5,6] with prototype filters of the same length.

The method in [3] has been omitted from the comparison because it requires a large amount of computation due to the repeated use of the Remez exchange algorithm, which makes this method impractical for applications where designs must be carried out in real or quasi-real time.

(1) *Reconstruction errors*: Fig. 8 shows plots of the percentage difference in the maximum reconstruction errors for the proposed method relative to that produced by the other two methods, which are given by

$$A = \frac{\max |e_m(\omega)|_{\text{other}} - \max |e_m(\omega)|_{\text{proposed}}}{\max |e_m(\omega)|_{\text{proposed}}} \times 100\%, \tag{22}$$

$$B = \frac{\max |e_a(\omega)|_{\text{other}} - \max |e_a(\omega)|_{\text{proposed}}}{\max |e_a(\omega)|_{\text{proposed}}} \times 100\%, \tag{23}$$

$$C = \frac{\max |e_{ta}(\omega)|_{\text{other}} - \max |e_{ta}(\omega)|_{\text{proposed}}}{\max |e_{ta}(\omega)|_{\text{proposed}}} \times 100\%. \tag{24}$$

When compared with the methods of [5,6], the proposed method was found to provide an average increase of 9.5% and 1.5% in the maximum amplitude error, an average increase of 0.01% and decrease of 0.01% in the maximum aliasing error, and an average increase of 0.06% and 0.04% in the maximum total aliasing error, respectively. While maximum amplitude error increased slightly for the proposed method, the aliasing errors were essentially unchanged.

(2) *Design time of the prototype filter*: The computation time required to design the prototype filter using the proposed method and the methods of [5,6] were 0.0470, 3.2868, and 7.6658 s, respectively. This is the worst-case scenario for the proposed method, which includes computational costs associated with the Kaiser window and spline interpolation for Eq. (20). In effect, the proposed method was found to reduce computational costs associated with the design of the prototype filter to 1.4% of that required by the method in [5] or to 0.6% of that required by the method in [6] on the average. This significant improvement is due to the fact that our solution is closed-form, whereas the methods of [5,6] require optimization routines to be performed.

5. Application to subband processing

Maximally decimated uniform filter banks like the proposed have been used extensively in audio coding [12] and have been incorporated into coding standards such as MPEG-1 [13] and MPEG-2 BC/LSF [14]. Effective coding depends heavily on

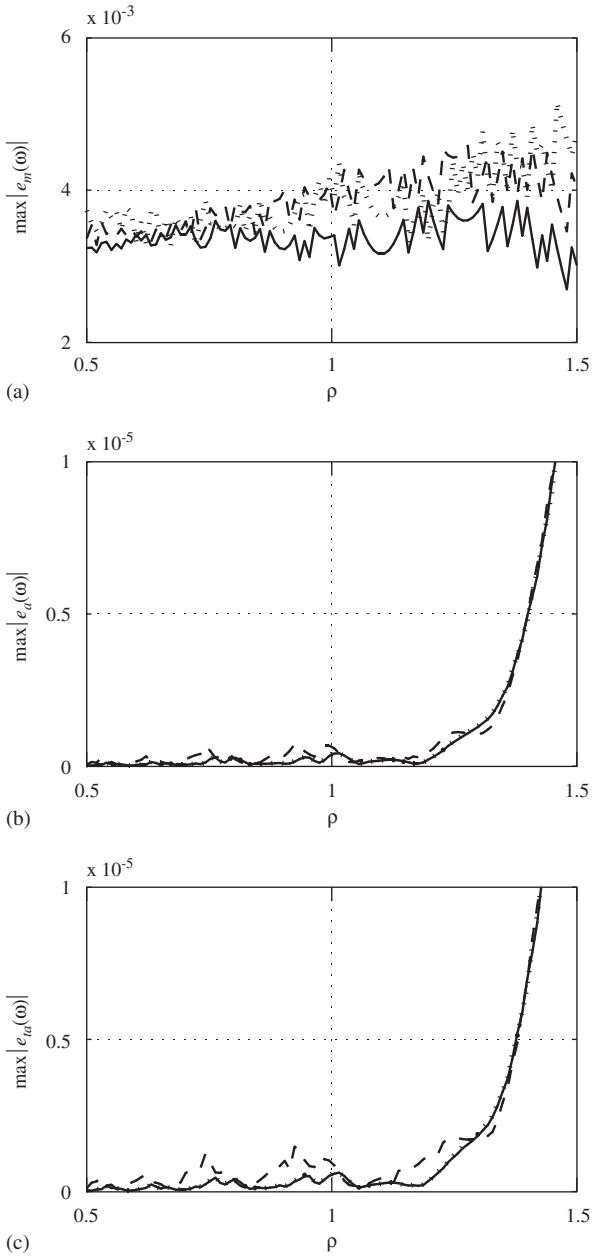

Fig. 6. Maximum reconstruction errors for a CMFB designed using the proposed method with $A_a = 100$ dB and $M = 32$ for the Kaiser (solid line), Saramäki (dotted line), and ultraspherical (dashed line) windows: (a) maximum amplitude distortion; (b) maximum aliasing distortion; and (c) maximum total aliasing distortion.

matching the properties of the analysis filter bank to the characteristics of the input signal [15]. Filter bank designers are confronted with a difficult time-frequency resolution trade-off and a poor resolution of this trade-off can lead to filter banks that cause

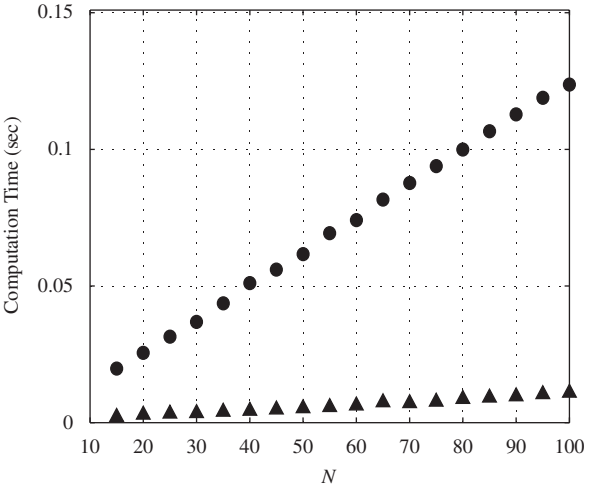

Fig. 7. Computation time associated with generating the coefficients of the ultraspherical (triangles) and Kaiser (circles) windows vs. the window length N.

undesirable artifacts. A piccolo calls for fine frequency resolution and coarse time resolution while a castanet's sound is highly time-localized and widely distributed in frequency. As a rule of thumb, audio signal models tend to remain constant for longer periods of time, e.g., for the duration of a song, and then change suddenly [16]. Consequently, adaptive filtering techniques, which can be computational intensive, may be replaced by an efficient filter-bank design method like the proposed, which can quickly match the analysis filter bank's time-frequency tiling to the spectrum of a new input signal. A detailed discussion on perceptual audio coding and filter bank matching can be found in [1] and the references therein.

In ECG processing, the filter bank approach provides an excellent framework for a variety of tasks including beat detection, signal enhancement, beat classification, and signal compression [2,17–19]. These tasks focus primarily on processing the P and T waves and the QRS complex, whose spectra extend up to 10 and 40 Hz, respectively. An input signal with frequency bandwidth from 0 to 180 Hz (input sampling rate of 360 Hz) can be decomposed using a 32-channel filter bank yielding uniform subbands {[0 to 5.625], [5.625 to 11.25],…, and [174.375 to 180]} Hz. In [2], a method for beat detection is described that employs the subbands containing the QRS complex (up to 40 Hz) while discarding the others. However, the time and frequency content of ECG signals can vary significantly depending on subject factors such as sex,

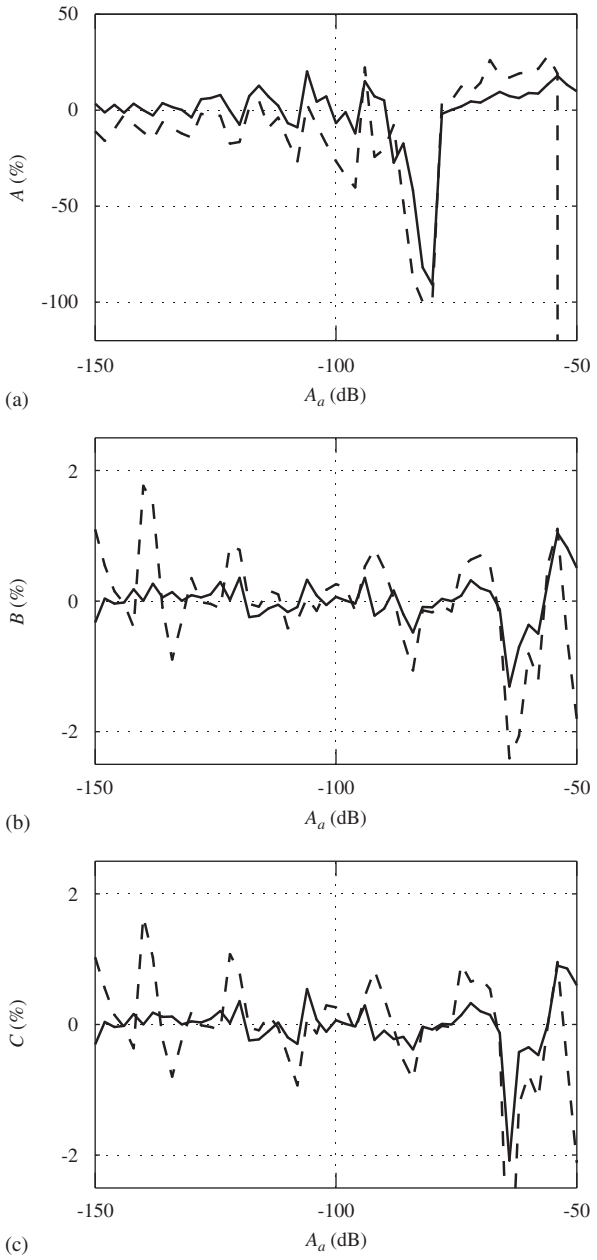

Fig. 8. Percentage difference in the maximum reconstruction errors for the proposed method relative to those produced by the methods of [5] (dashed line) and [6] (solid line): (a) amplitude error; (b) aliasing error; and (c) total aliasing error.

age, physical fitness, and activity during the time of recording [20–22]. For example, the duration of the QRS complex can range from 0.04 to 0.12 s and, as we will see in the following section, the stopband attenuation can have a significant effect on the fidelity of the reconstructed signal. As in the case of audio coding, an efficient filter-bank design method like the proposed can be used to quickly accommodate a variety of scenarios without requiring a considerable amount of computation. A detailed discussion on the processing of ECG signals can be found in [23].

5.1. Fidelity measures

The quality of a filter bank for subband processing can be evaluated by considering the fidelity of the reconstructed signal $y(n)$ to the original signal $x(n)$. The percent root-mean-square difference (PRD) is a fidelity measure given by [24]

$$\mathrm{PRD} = \left(\frac{\text{Reconstructed noise energy}}{\text{Original signal energy}}\right)^{1/2} \times 100\% = \left\{\frac{\sum_n [x(n)-y(n)]^2}{\sum_n [y(n)]^2}\right\}^{1/2} \times 100\%. \quad (25)$$

Two other measures include the mean square error (MSE) and maximum error (ME) given by

$$\mathrm{MSE} = \frac{1}{N}\sum_n |x(n)-y(n)|^2, \quad (26)$$

$$\mathrm{ME} = \max_n |x(n)-y(n)|. \quad (27)$$

Signal decomposition and reconstruction was carried out for speech, audio, and ECG signals. Speech and audio signals were obtained from the sound quality assessment material (SQAM) compact disc (CD) [25,26]. ECG recordings were obtained from the MIT-BIH Arrhythmia Database [27,28]. A 10-channel CMFB designed using the proposed method with a Kaiser window, stopband attenuation $A_a = 80$ dB, and roll-off factor $\rho = 1.00$ was used. Table 3 lists the PRD, MSE, and ME obtained for speech, audio, and ECG signals. As can be seen, the measures are consistent for all signal types. Average PRDs of 0.1224%, 0.1226%, and 0.1295% were obtained for the speech, audio, and ECG signals, respectively. PRDs in the range of 2–10% have been considered acceptable in practice [24]. Fig. 9 shows plots of the original MIT-BIH record 117 and its reconstructed version. It is observed that the filter bank does not distort features of the ECG signal. Similarly, differences between the original and reconstructed speech and audio signals could not be discerned during listening tests.

Table 3
Distortion for signal decomposition and reconstruction for filter bank with $M = 10$, $A_a = 80\,\text{dB}$, and $\rho = 1.00$

Signal	PRD	MSE	ME
SQAM Trk. 49: Speech, F, Eng.	1.224×10^{-1}	8.032×10^{-9}	6.080×10^{-4}
SQAM Trk. 50: Speech, M, Eng.	1.218×10^{-1}	1.120×10^{-8}	8.863×10^{-4}
SQAM Trk. 51: Speech, F, Fre.	1.249×10^{-1}	1.483×10^{-8}	9.400×10^{-4}
SQAM Trk. 52: Speech, M, Fre.	1.319×10^{-1}	1.199×10^{-8}	9.393×10^{-4}
SQAM Trk. 53: Speech, F, Ger.	1.107×10^{-1}	5.283×10^{-9}	5.285×10^{-4}
SQAM Trk. 54: Speech, M, Ger.	1.230×10^{-1}	6.479×10^{-9}	6.840×10^{-4}
SQAM Trk. 21: Trumpet	1.278×10^{-1}	2.257×10^{-9}	1.874×10^{-4}
SQAM Trk. 23: Horn	1.091×10^{-1}	1.353×10^{-8}	4.303×10^{-4}
SQAM Trk. 35-2: Glockenspiel	1.285×10^{-1}	7.123×10^{-9}	7.699×10^{-4}
SQAM Trk. 40: Harpsichord	1.251×10^{-1}	1.601×10^{-9}	3.260×10^{-4}
MIT-BIH Rec. 106: F, 24, Norm.	1.295×10^{-1}	2.386×10^{-8}	9.978×10^{-4}
MIT-BIH Rec. 117: M, 69, Norm.	1.415×10^{-1}	6.637×10^{-7}	1.961×10^{-3}
MIT-BIH Rec. 217: M, 65, Ab.	1.294×10^{-1}	2.978×10^{-7}	1.325×10^{-3}
MIT-BIH Rec. 232: F, 76, Ab.	1.178×10^{-1}	3.951×10^{-8}	1.013×10^{-3}

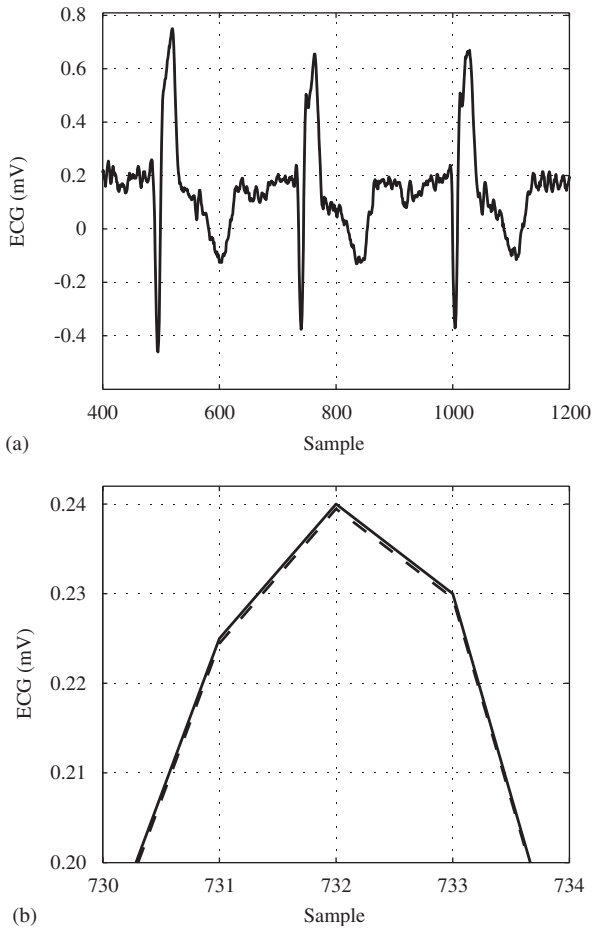

Fig. 9. MIT-BIH ECG record 117. Original signal (solid line) and reconstructed signal (dashed line): (a) record over three heartbeats; (b) a zoomed in version of the record.

To examine the effects of the stopband attenuation on the measures, 10-channel CMFBs (Kaiser window) with $\rho = 1.00$ were designed for the range $A_a = [-150, -50]\,\text{dB}$. Fig. 10 shows plots of the measures for MIT-BIH record 117. The measures remain relatively unchanged throughout the region $A_a = [-150, -75]\,\text{dB}$ and begin to increase by one order of magnitude through the region $A_a = [-75, -50]\,\text{dB}$. On the other hand, the MSE increases approximately two orders of magnitude. Similar results were found for other test signals.

To examine the effects of the roll-off ratio on the measures, 10-channel CMFBs (Kaiser window) with $A_a = -80\,\text{dB}$ were designed for the range $\rho = [0.5, 1.5]$. Fig. 11 shows plots of the measures for MIT-BIH record 117. Small fluctuations (of the same order of magnitude) were observed for the measures. Average values for the PRD, MSE, and ME were 0.1126%, 5.41×10^{-7}, and 1.77×10^{-3}, respectively.

6. Conclusions

An efficient closed-form window method for designing prototype filters for M-channel CMFBs was proposed. The method is based on empirical formulas that give the required filter length and window parameters that would satisfy the prescribed stopband attenuation and roll-off factor. Experimental results have shown that, on the average, the Kaiser window yields the smallest reconstruction error relative to that achieved with

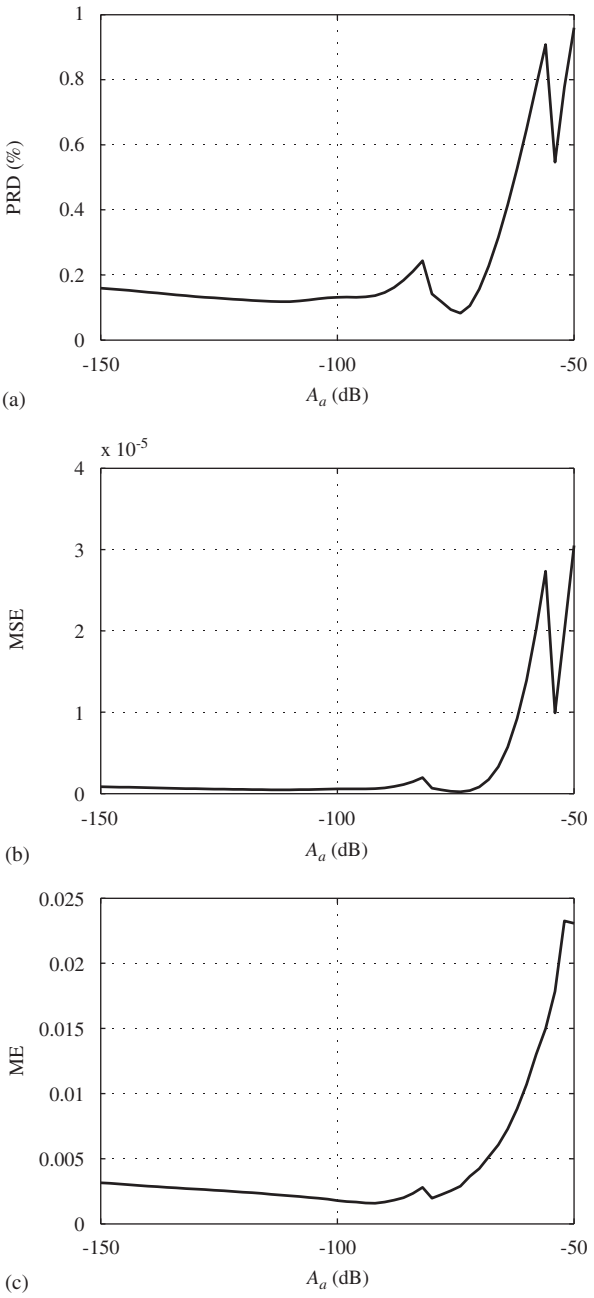

Fig. 10. Distortion for the signal decomposition and reconstruction process achieved for filter banks designed using the proposed method with the Kaiser window, $M = 10$, $\rho = 1.00$, and various values of the stopband attenuation. The MIT-BIH record 117 was used for all tests: (a) percent root-mean-square difference; (b) mean square error; and (c) maximum error.

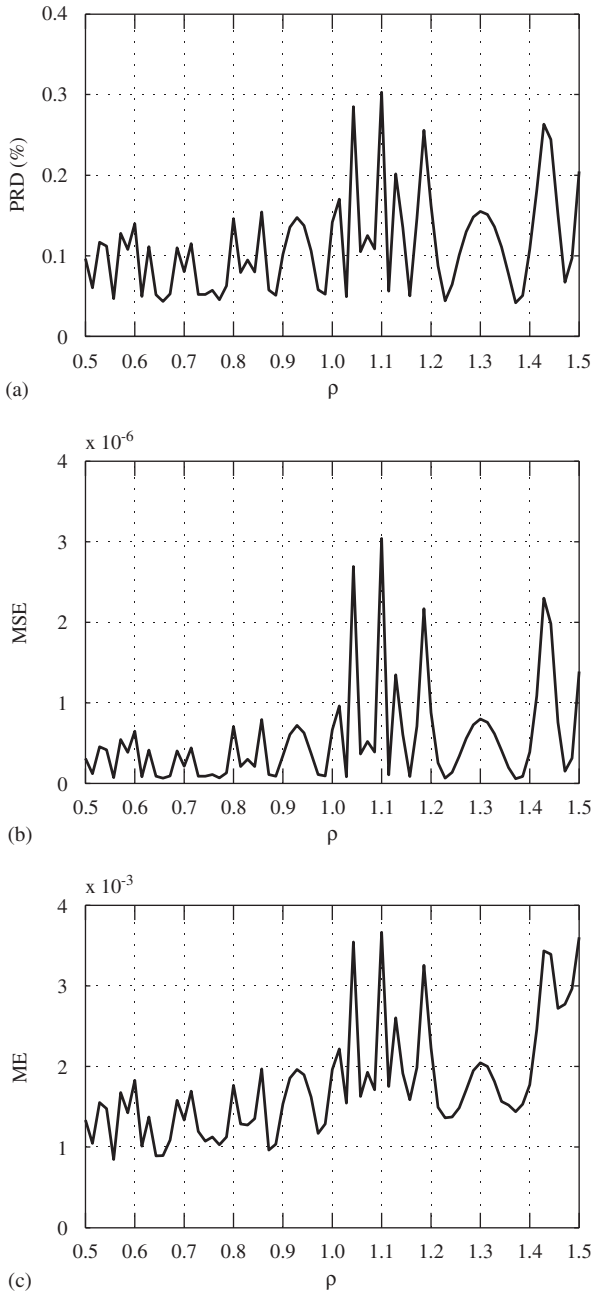

Fig. 11. Distortion for the signal decomposition and reconstruction process achieved for filter banks designed using the proposed method with the Kaiser window, $M = 10$, $A_a = -80\,\mathrm{dB}$, and various values of the roll-off ratio. The MIT-BIH record 117 was used for all tests: (a) percent root-mean-square difference; (b) mean square error; and (c) maximum error.

designs obtained using the Saramäki or ultraspherical window. On the other hand, the use of the ultraspherical window reduces the length of the prototype filter by 3.1% and the amount of computation associated with the design of the prototype filter by 9.3%, on the average, when compared with designs obtained using the Kaiser window. A comparison has shown that the amount

of computation required by the proposed method is a small fraction less than 2% relative to that required by the methods in [5,6], the aliasing error is approximately the same, but the amplitude error is slightly larger. The low computational complexity renders the proposed method highly suitable for applications where the design must be carried out in real or quasi-real time.

References

[1] T. Painter, A. Spanias, Perceptual coding of digital audio, Proceedings of IEEE, vol. 88(4), April 2000, pp. 451–513.

[2] V.X. Afonso, W.J. Tompkins, T.Q. Nguyen, S. Luo, ECG beat detection using filter banks, IEEE Trans. Biomed. Eng. 46 (2) (February 1999) 192–202.

[3] C.D. Creusere, S.K. Mitra, A simple method for designing high-quality prototype filters for M-band pseudo QMF banks, IEEE Trans. Signal Process. 34 (4) (April 1995) 1005–1007.

[4] A. Antoniou, Digital Signal Processing: Signals, Systems, and Filters, McGraw-Hill, New York, NY, USA, 2005.

[5] Y.-P. Lin, P.P. Vaidyanathan, A Kaiser window approach for the design of prototype filters of cosine modulated filterbanks, IEEE Signal Process. Lett. 5 (6) (June 1998) 132–134.

[6] F. Cruz-Roldán, P. Amo-Lopez, S. Maldonado-Bascon, S.S. Lawson, An efficient and simple method for designing prototype filters for cosine-modulated pseudo-QMF banks, IEEE Signal Process. Lett. 9 (1) (January 2002) 132–134.

[7] T. Saramäki, A class of window functions with nearly minimum sidelobe energy for designing FIR filters, IEEE International Symposium on Circuits and Systems, vol. 1, Portland, OR, USA, May 1989, pp. 359–362.

[8] S.W.A. Bergen, A. Antoniou, Design of nonrecursive digital filters using the ultraspherical window function, EURASIP J. Appl. Signal Process. 2005 (12) (2005) 1910–1922.

[9] P.P. Vaidyanathan, Multirate Systems and Filter Banks, Prentice-Hall, Englewood Cliffs, NJ, 1993.

[10] T. Saramäki, R. Bregović, Multirate systems and filter banks, in: G. Jovanovic-Dolecek (Ed.), Multirate Systems: Design & Applications, Idea Group Publishing, Hershey, PA, USA, 2002.

[11] R. Fletcher, Practical Methods of Optimization, Wiley, New York, NY, USA, 1987.

[12] M. Vetterli, J. Kovačević, Wavelets and Subband Coding, Prentice-Hall, Englewood Cliffs, NJ, USA, 1995.

[13] ISO/IEC, JTC1/SC29/WG11 MPEG, Information technology—coding of moving pictures and associated audio for digital storage media at up to about 1.5 Mbits/s—part 3: audio, IS11172-3, 1992 (“MPEG-1”).

[14] ISO/IEC, JTC1/SC29/WG11 MPEG, Information technology—generic coding of moving pictures and associated audio, IS13818-3, 1994 (“MPEG-2”).

[15] J. Johnston, S. Quackenbush, G. Davidson, K. Brandenburg, J. Herre, MPEG audio coding, in: A. Akansu, M. Medley (Eds.), Wavelet, Subband, and Block Transforms in Communications and Multimedia, Kluwer Academic Publishers, Boston, MA, USA, 1999.

[16] J. Johnston, Audio coding with filter banks, in: A. Akansu, M.J.T. Smith (Eds.), Subband and Wavelet Transforms, Kluwer Academic Publishers, Boston, MA, USA, 1996.

[17] V.X. Afonso, W.J. Tompkins, T.Q. Nguyen, K. Michler, S. Luo, Comparing stress ECG enhancement algorithms: with an introduction to a filter bank based approach, IEEE Eng. Med. Biol. Mag. 15 (3) (1996) 37–44.

[18] M.C. Aydin, A.E. Cetin, H. Koymen, ECG data compression by sub-band coding, Electron. Lett. 27 (4) (1991) 359–360.

[19] A.E. Cetin, H. Koymen, M.C. Aydin, Multichannel ECG data compression by multirate signal processing and transform domain coding techniques, IEEE Trans. Biomed. Eng. 40 (5) (1993) 495–499.

[20] J.A. Larsen, A.H. Kadish, Effects of gender on cardiac arrhythmias, J. Cardiovasc. Electrophysiology 9 (6) (1998) 655–664.

[21] H.V. Huikuri, S.M. Pikkujamsa, K.E.J. Airaksinen, M.J. Ikaheimo, A.O. Rantala, H. Kauma, M. Lilja, Y.A. Kesaniemi, Sex-related differences in autonomic modulation of heart rate in middle-aged subjects, Circulation 94 (1996) 122–125.

[22] G.J. Taylor, 150 Practice ECGs: Interpretation and Review, third ed., Blackwell Publishing, Malden, MA, USA, 2006.

[23] W.J. Tompkins (Ed.), Biomedical Digital Signal Processing: C-Language Examples and Laboratory Experiments for the IBM PC, Prentice-Hall, Englewood Cliffs, NJ, USA, 1993.

[24] S.M.S. Jalaleddine, C.G. Hutchens, R.D. Strattan, W.A. Coberly, ECG data compression techniques—a unified approach, IEEE Trans. Biomed. Eng. 37 (4) (April 1990) 329–343.

[25] European Broadcasting Union (EBU), Sound Quality Assessment Material (SQAM) Compact Disc, Geneva, Switzerland, 1988.

[26] K. Brandenburg, R. Henke, Near-lossless coding of high quality digital audio: first results, IEEE International Conference on Acoustics, Speech, and Signal Processing, vol. 1, Minneapolis, MN, USA, April 1993, pp. 193–196.

[27] R.G. Mark, P.S. Schluter, G.B. Moody, P. Devlin, D. Chernoff, An annotated ECG database for evaluating arrhythmia detectors, IEEE Engineering in Medicine and Biology Society Conference, vol. 1, 1982, pp. 205–210.

[28] G.B. Moody, R.G. Mark, The impact of the MIT-BIH Arrhythmia Database, IEEE Eng. Med. Biol. Mag. 20 (3) (May/June 2001) 45–50.